AJNR

Clinical positron emission tomography for brain tumors: comparison of fludeoxyglucose F 18 and L-methyl-11C-methionine.

T Ogawa, A Inugami, J Hatazawa, I Kanno, M Murakami, N Yasui, K Mineura and K Uemura

AJNR Am J Neuroradiol 1996, 17 (2) 345-353
http://www.ajnr.org/content/17/2/345

Clinical Positron Emission Tomography for Brain Tumors: Comparison of Fludeoxyglucose F 18 and L-Methyl-^{11}C-methionine

Toshihide Ogawa, Atsushi Inugami, Jun Hatazawa, Iwao Kanno, Matsutaro Murakami, Nobuyuki Yasui, Katsuyoshi Mineura, and Kazuo Uemura

PURPOSE: To evaluate the differences between fludeoxyglucose F 18 (FDG) and L-methyl-^{11}C-methionine (^{11}C-methionine) as tracers for positron emission tomography (PET) in the evaluation of brain tumors. **METHODS:** We analyzed 10 patients with histologically verified cerebral glioma or meningioma and 1 patient with a neuroradiologic diagnosis of low-grade glioma by using FDG, ^{11}C-methionine, and PET. We qualitatively and quantitatively evaluated the extent and degree of accumulation of FDG and ^{11}C-methionine in the tumor tissue. **RESULTS:** Although PET with FDG depicted malignant tumors as a hot spot in all cases, it was not able to delineate the extent of the tumor. Conversely, PET with ^{11}C-methionine outlined the tumors as areas of increased accumulation of ^{11}C-methionine, regardless of the degree of malignancy. **CONCLUSION:** PET with FDG and with ^{11}C-methionine can play complementary roles in the evaluation of brain tumors.

Index terms: Brain neoplasms, radionuclide studies; Positron emission tomography

AJNR Am J Neuroradiol 17:345–353, February 1996

Positron emission tomography (PET) has provided valuable biophysiological information on various central nervous system disorders. In brain tumors, various radiotracers have been applied with PET to evaluate tumor blood flow and metabolism, as well as to detect tumors and to assess the degree of malignancy (1–4). Among the various radiotracers, fludeoxyglucose F 18 (FDG) has been the most frequently used for the evaluation of glucose metabolism in brain tumors. In addition, the assessment of tumor protein synthesis has been attempted with various amino acid tracers, and the most experience has been obtained with L-methyl-^{11}C-methionine (^{11}C-methionine) (3, 5–7). In a few studies both FDG and ^{11}C-methionine have been applied to tumors (8–10). In the present study, we applied both tracers to patients with glioma or meningioma to evaluate the differences of FDG and ^{11}C-methionine as radiotracers for brain tumors.

Received March 1, 1995; accepted after revision August 10.

Supported by Grant-in-Aid 04151070 for cancer research from the Ministry of Education, Science, and Culture, Japan.

From the Departments of Radiology and Nuclear Medicine (T.O., A.I., J.H., I.K., M.M., K.U.) and Surgical Neurology (N.Y.), Research Institute of Brain and Blood Vessels—Akita, and Department of Neurosurgical Service, Akita University School of Medicine (K.M.), Akita City, Akita, Japan.

Address reprint requests to Toshihide Ogawa, MD, Department of Radiology and Nuclear Medicine, Research Institute of Brain and Blood Vessels—Akita, 6-10, Senshu-kubota-machi, Akita City, 010, Akita, Japan.

AJNR 17:345–353, Feb 1996 0195-6108/96/1702–0345

Subjects and Methods

Subjects

We used PET with FDG and ^{11}C-methionine to examine 16 patients who were clinically thought to have brain tumors. Five of them were confirmed to have radiation injury, and, as in our previous report on this group (11), we excluded these 5 from the present analysis and assessed the other 11 patients (6 men and 5 women) (Table 1). The patients ranged in age from 29 to 67 years (mean, 48 years). Pathologic verification was obtained in 10 patients (5 had low-grade glioma, 4 had high-grade glioma, and 1 had meningioma), and in the remaining patient, low-grade glioma was diagnosed from the neuroradiologic data.

Methods

PET was carried out with Headtome IV PET scanners (Shimadzu, Kyoto, Japan). The Headtome IV scanner provides 14 images with 6.5-mm intervals and a spatial resolution of 4.5-mm full width at half maximum in the imaging plane (12). PET was performed parallel to the orbitomeatal line.

After a transmission scan was obtained, a dose of 185 to 333 MBq (5 to 9 mCi) of FDG or 740 to 2220 MBq (30 to 60 mCi) of ^{11}C-methionine was intravenously injected into the cubital vein within 1 minute. Static scanning was performed for a 12-minute period at 60 minutes after the FDG injection. Arterial blood samples were obtained periodically after the injection of FDG. For PET with ^{11}C-methionine, a 12-minute static scan using the Headtome IV was begun 30 minutes after ^{11}C-methionine injection. No arterial blood samples were obtained for PET with ^{11}C-methionine. The interval between PET with FDG and PET with ^{11}C-methionine was less than 1 week (mean, 4.5 days).

Before the first PET scan, a CT/T 9800 scanner (GE Medical Systems, Milwaukee, Wis) was used to obtain computed tomographic (CT) scans both before and after the injection of iopamidol. Scans were obtained parallel to the orbitomeatal line with a 10-mm section thickness and 6.5-mm section interval. The method of achieving accurate alignment between CT and PET studies has been previously reported in detail (13, 14). Magnetic resonance (MR) imaging was also performed before and after injection of gadopentteate dimeglumine with a 0.5-T superconducting MR unit (Magnex 50, Shimadzu) in six patients before the second PET examination. Informed consent for the PET studies was obtained from the patients or their relatives. This project was approved by the Committee for Clinical PET Study of the Research Institute of Brain and Blood Vessels—Akita.

Data Analysis

We evaluated the accumulation of FDG and ^{11}C-methionine in tumor tissue both qualitatively and quantitatively. Tracer accumulation was divided into three grades (lower, similar, and higher) by comparison with the accumulation in the contralateral gray matter. For a quantitative analysis of FDG uptake, the metabolic rate for glucose (MRGlu) was assessed by the FDG method of Phelps et al (15). The MRGlu was calculated by using fixed-rate constants from healthy volunteers and a lumped constant of 0.52 (16). To assess ^{11}C-methionine uptake, we evaluated the concentration of ^{11}C-methionine at 36 minutes after injection on the basis of the differential absorption ratio (DAR) (17) of tumor tissue. The DAR was calculated as follows: DAR = [(pixel count/pixel volume)/(injected radioisotope activity/body weight)] $\times$ calibration factor, where the calibration factor denotes the ratio of the counts recorded by the PET camera to those of a well counter. By superimposing a CT scan on the corresponding PET image, we defined a region of interest (ROI) in the tumor tissue and calculated the MRGlu and DAR of ^{11}C-methionine in the same location. A round ROI 16 to 24 mm in diameter was located in the tumor, depending on the tumor's size. When the tumor showed enhancement on CT scans, we set the ROI on the enhanced region. When the tumor showed no enhancement on CT scans, we set the ROI on the homogeneous solid component but avoided areas of calcification. We compared the MRGlu and the DAR of ^{11}C-methionine in the tumors by using linear regression analysis.

TABLE 1: Clinical data of patients

Patient	Age, y/ Sex	Location of Tumor	Histology
1	29/M	L frontal	Astrocytoma grade 2
2	40/F	R frontal	Astrocytoma grade 2
3	67/M	R frontotemporoparietal	Astrocytoma grade 2
4	33/M	R frontal, basal ganglia	Oligodendroglioma grade 2
5	53/M	R lateral ventricle	Central neurocytoma
6	41/F	Brain stem	(low-grade glioma)*
7	61/F	Bilateral frontal	Meningioma
8	57/M	R temporoparietal	Malignant astrocytoma grade 3
9	31/F	L frontal	Malignant astrocytoma grade 3
10	54/M	L frontal	Glioblastoma multiforme
11	67/F	R frontal	Glioblastoma multiforme

* Histology not available. This case was neuroradiologically diagnosed as low-grade glioma.

TABLE 2: Qualitative and quantitative data from positron emission tomographic studies

Patient	Degree of Accumulation in Tumor Tissue		Area of Accumulation in Tumor Tissue	Quantitative Evaluation of Accumulation in Tumor Tissue	
	FDG	Met		MRGlu (mg/100 mL/min)	DAR of Met
1	−	++	. . .	3.04	2.16
2	−	++	. . .	1.81	1.49
3	−	+	. . .	3.20	1.97
4	−	++	. . .	2.75	2.24
5	+	++	FDG < Met	3.89	1.80
6	−	++	. . .	3.99	3.29
7	−	+	. . .	1.97	1.61
8	++	++	FDG < Met	5.84	4.17
9	+	++	FDG < Met	3.80	2.22
10	+	++	FDG < Met	5.78	3.29
11	++	++	FDG < Met	10.40	5.71

Note.—FDG indicates fludeoxyglucose F 18; Met, L-methyl-^{11}C-methionine; MRGlu, metabolic rate of glucose; DAR, differential absorption ratio; −, uptake less than in gray matter; +, uptake almost the same as in gray matter; ++, uptake greater than in gray matter; <, markedly less than.

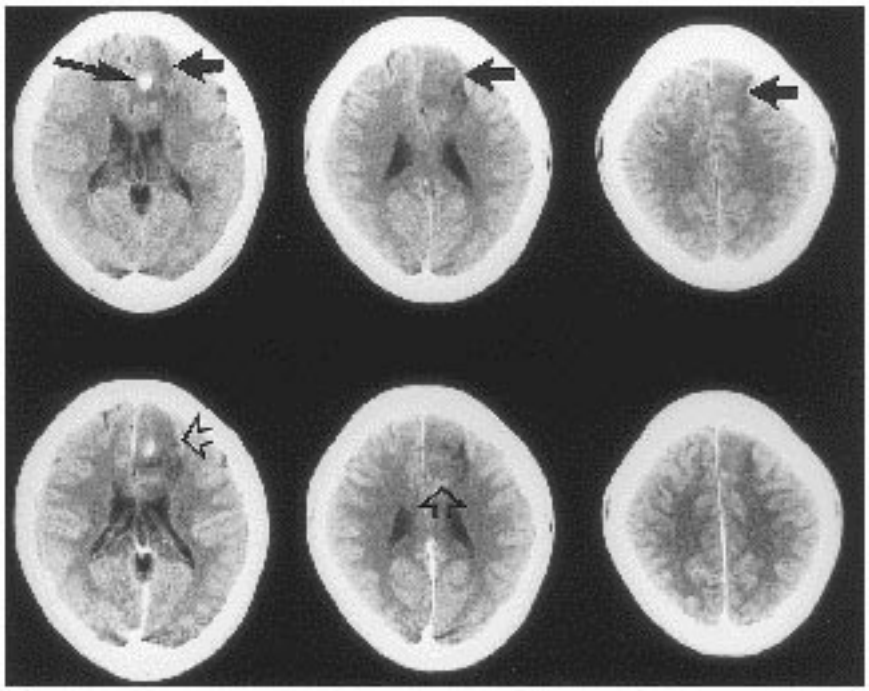

A

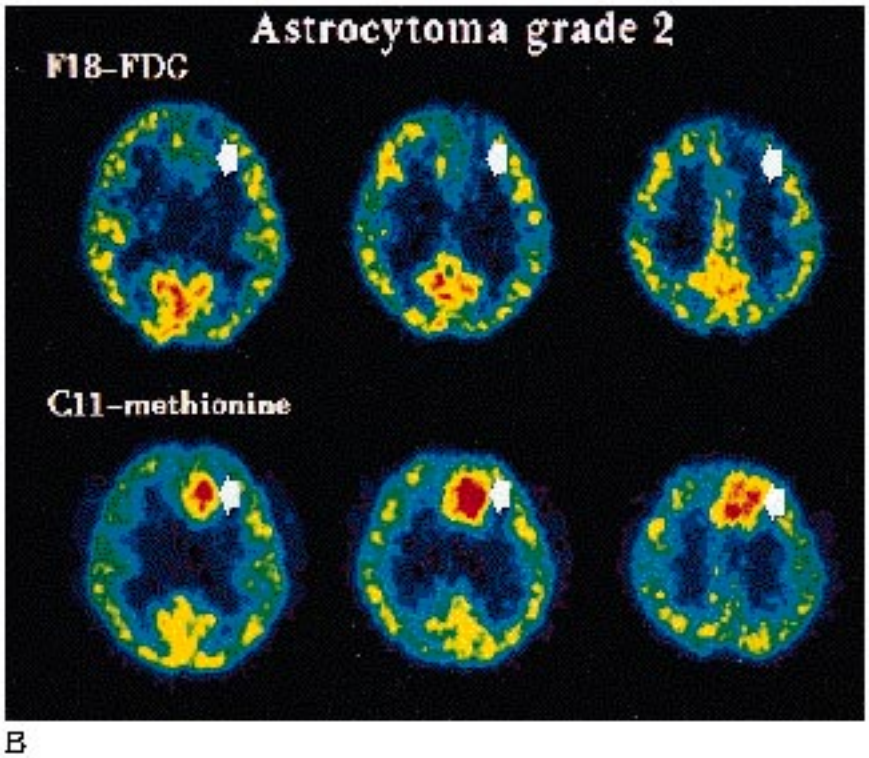

B

Fig 1. Patient 1. Astrocytoma, grade 2.

A, Unenhanced CT scans (*upper*) show a round area of low attenuation (*short arrows*) with a small nodule of calcification (*long arrow*) in the medial frontal region. Contrast-enhanced CT scans (*lower*) show faint ringlike enhancement (*open arrows*) around the mass.

B, PET with FDG scans (*upper*) show a hypometabolic area in the left medial frontal region (*arrows*). PET with ^{11}C-methionine scans (*lower*) show markedly increased accumulation of ^{11}C-methionine in the left frontal lobe tumor (*arrows*).

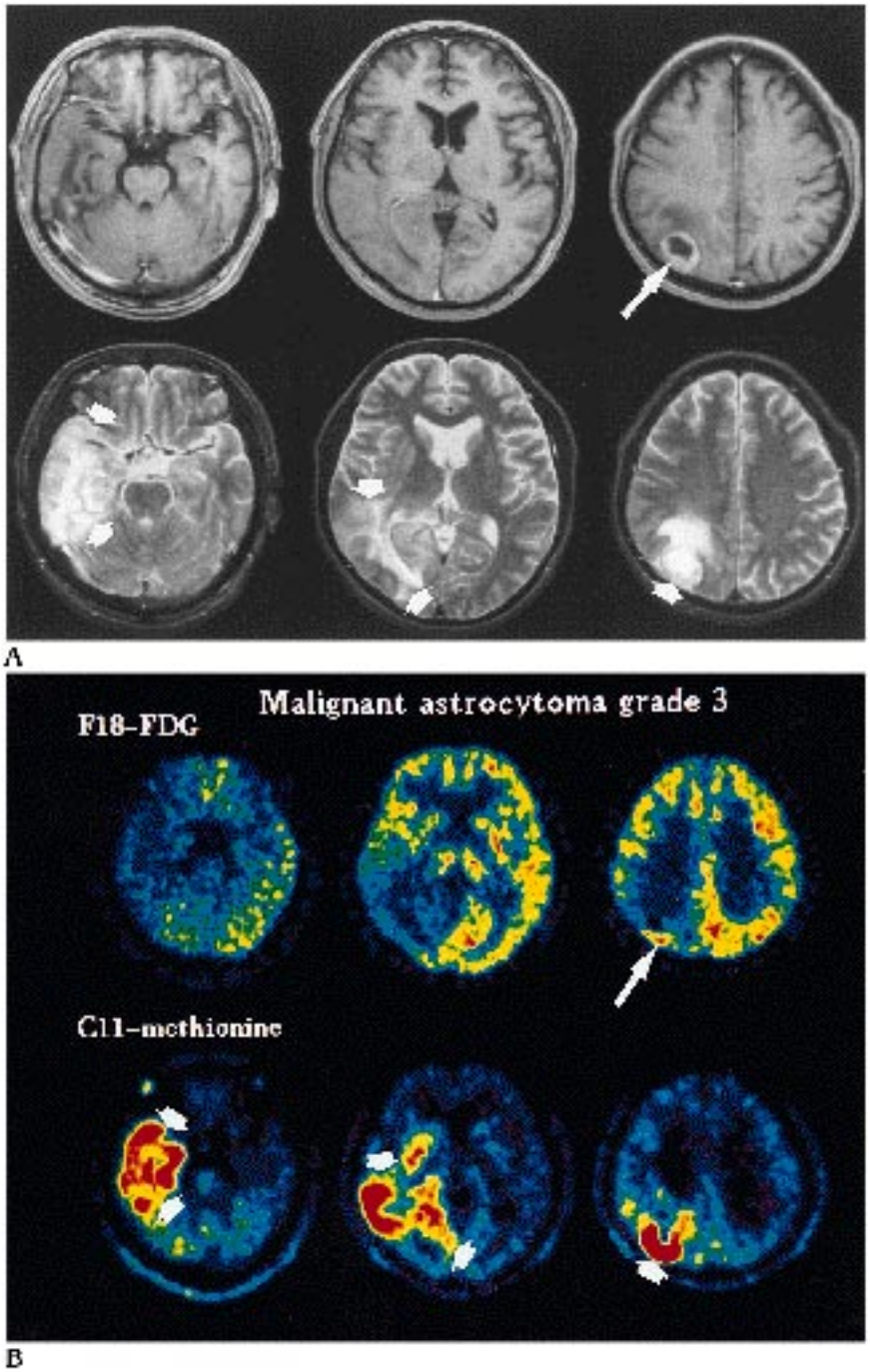

Fig 2. Patient 8. Malignant astrocytoma, grade 3.

A, Contrast-enhanced T1-weighted gradient-echo MR images (420/10 [repetition time/echo time], 90° flip angle) (*upper*) show ringlike enhancement around the round mass (*long arrow*) in the right parietal lobe. T2-weighted spin-echo MR images (3000/90) (*lower*) show an extensive hyperintense area mainly involving the white matter in the right temporoparietooccipital region (*short arrows*).

B, PET scans with FDG (*upper*) show a hypermetabolic focus (*long arrow*) that corresponds to the enhancing lesion on MR images and a surrounding hypometabolic area. PET scans with ^{11}C-methionine (*lower*) show an area of ^{11}C-methionine accumulation in the right temporoparietooccipital region (*short arrows*) extending to the right basal ganglia. *Figure continues.*

Results

Table 2 summarizes the qualitative and quantitative data for PET with FDG and for PET with ^{11}C-methionine. PET with FDG showed FDG hypometabolism in tumor tissue as compared with the contralateral gray matter in all patients with low-grade glioma or meningioma except one (patient 5). In patients with high-grade glioma, PET with FDG showed FDG hypermetabolism in the tumors of all patients. Conversely, PET with ^{11}C-methionine showed equal or increased accumulation in the tumors of all patients regardless of the grade of malignancy (Figs 1–3). The degree of accumulation in the tumor tissue was greater than in the adjacent and contralateral gray matter in nine patients. In the remaining two patients (who had low-grade glioma and meningioma, respectively), the accumulation in the tumor tissue was almost the same as that in the gray matter. In one patient with meningioma, PET with ^{11}C-methionine showed an increased accumulation in the enhancing part of the tumor but no increase of accumulation in the surrounding edema. In one patient with a low-grade glioma and four patients with high-grade gliomas, PET showed increased tumor accumulation of both tracers, but the area of increased accumulation of ^{11}C-methionine was larger than that for FDG (Figs 2 and 3).

Quantification of FDG accumulation showed that the MRGlu of high-grade gliomas was significantly higher than that of low-grade tumors ($P < .02$, Student's t test) (Table 3). The DAR of ^{11}C-methionine was also significantly higher for high-grade gliomas than for low-grade tumors ($P < .02$, Student's t test) (Table 3). A good correlation was found between the MRGlu and DAR values of tumor tissue by linear regression ($P < .001$) (Fig 4).

Discussion

PET with FDG has been widely used for the evaluation of many different types of tumor. Since Di Chiro et al (1) used PET with FDG to show that the glucose utilization of tumor tissue was correlated with the degree of malignancy, the clinical usefulness of this technique for brain tumors has been generally accepted. Clinical studies of brain tumors with PET and FDG have shown that it is useful for evaluating tumor grade, selecting a site for stereotaxic biopsy, evaluating the prognosis and the response to treatment, and distinguishing between recurrence and radiation necrosis (18–26).

In this study, PET with FDG showed hypometabolic foci in all but one patient with low-grade glioma and meningioma, and it showed a visible focus of FDG hypermetabolism in four patients with high-grade glioma. PET with FDG was thus helpful for distinguishing between low-grade and high-grade tumors, except in one patient. Malignant glioma, especially glioblastoma multiforme, usually shows regional histologic heterogeneity. Whole-brain sections con-

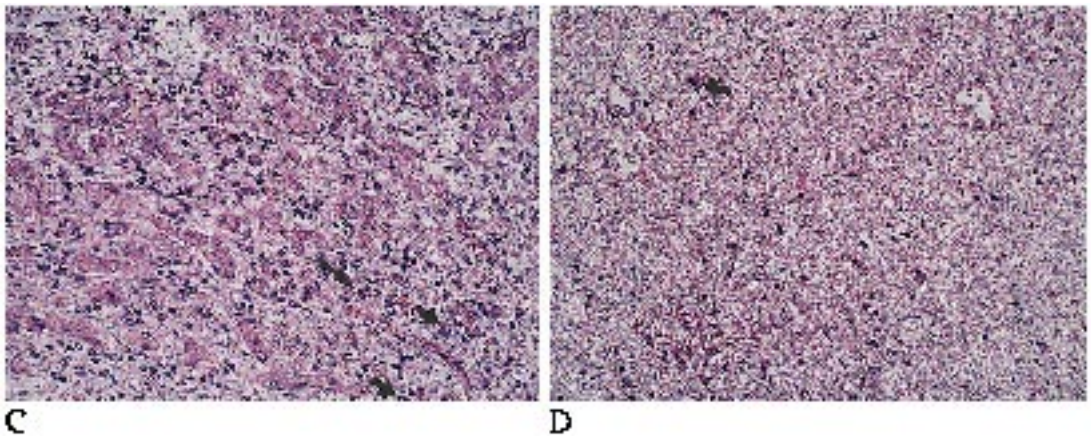

Fig 2, *continued.*

C, Histology of the enhancing lesion in the right parietal lobe on MR imaging revealed grade 3 malignant astrocytoma from the findings of increased cellularity, polymorphism of the tumor cells (*short arrows*), mitotic figures (*long arrow*), and proliferation of the blood vessels with glomeruloid appearance (*open arrows*) (hematoxylin-eosin, magnification ×200).

D, Histology of the temporal and occipital lobes gave a diagnosis of low-grade astrocytoma from the presence of tumor cells with nuclear atypism (*arrow*) (hematoxylin-eosin, magnification ×200).

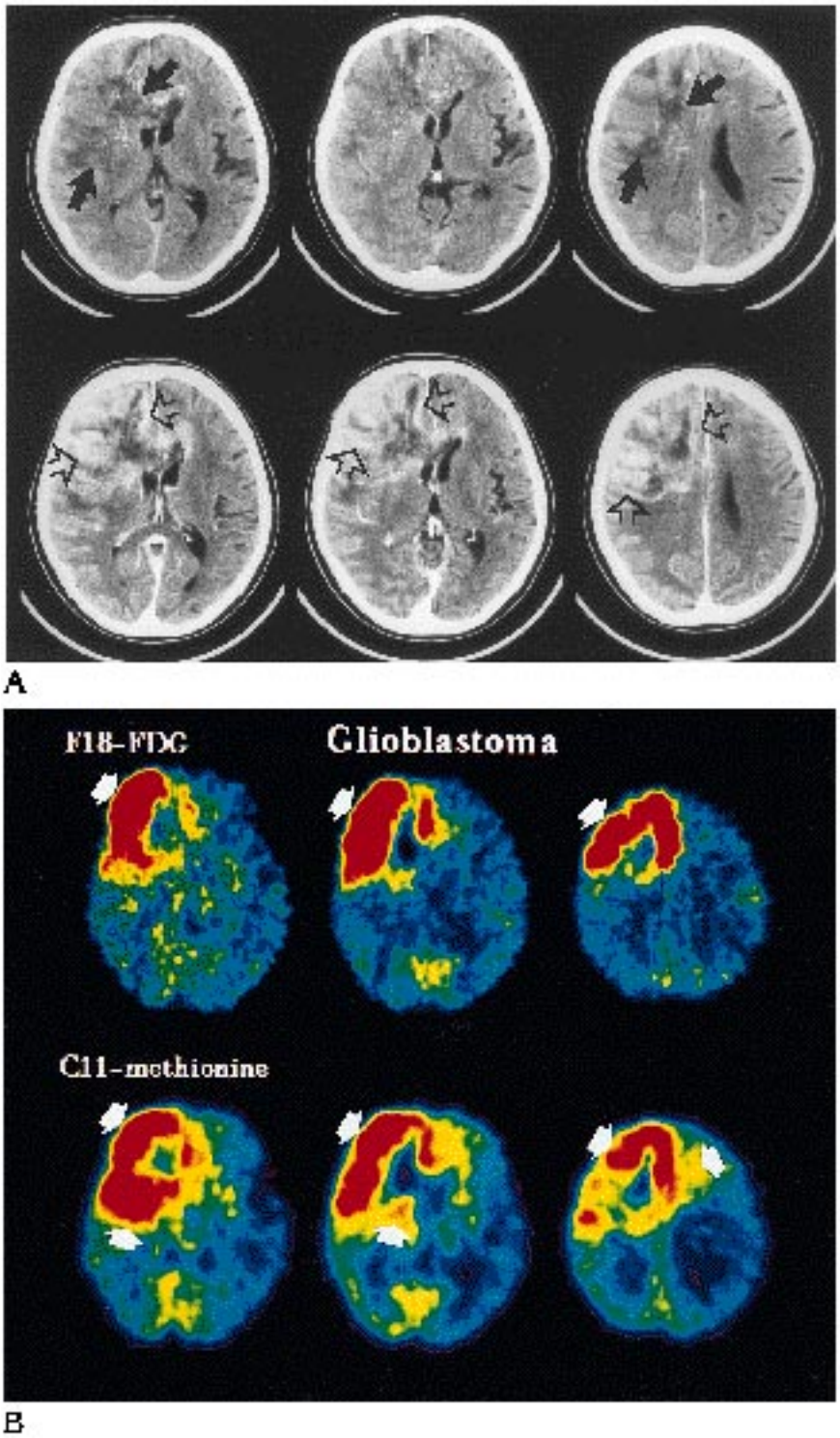

Fig 3. Patient 11. Glioblastoma multiforme.

A, Unenhanced CT scans (*upper*) show a poorly defined area of low attenuation (*closed arrows*) with many tiny calcified foci in the right frontal lobe and basal ganglia extending to the corpus callosum. Contrast-enhanced CT scans (*lower*) show irregular enhancement in the right frontal lobe (*open arrows*) extending to the left frontal lobe through the corpus callosum.

B, PET with FDG images (*upper*) show marked FDG hypermetabolism in the right frontal lobe tumor (*arrows*) extending to the left frontal lobe. The area of increased accumulation of ^{11}C-methionine (*arrows*) (*lower*) is slightly larger than that of FDG, hypermetabolism.

TABLE 3: Summary of MRGlu and DAR of L-methyl-^{11}C-methionine of low-grade and high-grade tumor tissue

Tumor Grade	MRGlu (mg/100 mL/min)	DAR of L-Methyl-^{11}C-methionine
Low grade (n = 7)	3.0 ± 0.9	2.1 ± 0.6
High grade (n = 4)	6.5 ± 2.8	3.8 ± 1.5

Note.—MRGlu indicates metabolic rate for glucose; DAR, differential absorption rate of L-methyl-^{11}C-methionine. Values are expressed as mean ± standard deviation. The difference between the values for low-grade tumors and the values for high-grade tumors is statistically significant ($P < .02$, according to Student's t test).

tain a mixture of well-differentiated and poorly differentiated cells within the same glioblastoma multiforme lesion (27). Although the principal features that distinguish low-grade astrocytomas from high-grade astrocytomas are cellularity and pleomorphism (28), Herholz et al (29) found that tumor cell density was a major determinant of astrocytoma glucose consumption. As we showed in the present study, metabolic imaging with FDG was useful for detecting malignant foci in highly heterogeneous tumors. However, it was difficult to evaluate tumor extent on PET scans with FDG.

Most reports have stressed that PET with ^{11}C-methionine can achieve better delineation of tumor tissue than CT scanning can (4, 5, 30–32). In this study, PET with ^{11}C-methionine clearly delineated the tumor extent regardless of the grade of malignancy. Although it was difficult to distinguish high-grade glioma from low-grade tumors by means of visual assessment, ^{11}C-methionine showed greater accumulation in the malignant focus of each high-grade glioma. This was confirmed by the DAR data for tumor tissue: DAR values tended to be higher for high-grade glioma. ^{11}C-methionine did not show increased accumulation in the edema surrounding meningioma, but it did accumulate in the presumed edematous tissue as shown on MR scans used during surgery to show tumor infiltration (Fig 2). It is difficult to distinguish tumor infiltration from spreading vasogenic edema even with MR imaging (33). Mosskin et al (31) reported that PET with ^{11}C-methionine was more accurate than CT or MR imaging for assessing the extent of viable tumor tissue (31). Although we cannot draw any definite conclusions from this small number of patients about whether PET with ^{11}C-methionine is superior to MR imaging for evaluating tumor extent, it appears to be useful for detecting tumor infiltration into regions presumed to be edematous on the basis of CT and MR imaging findings.

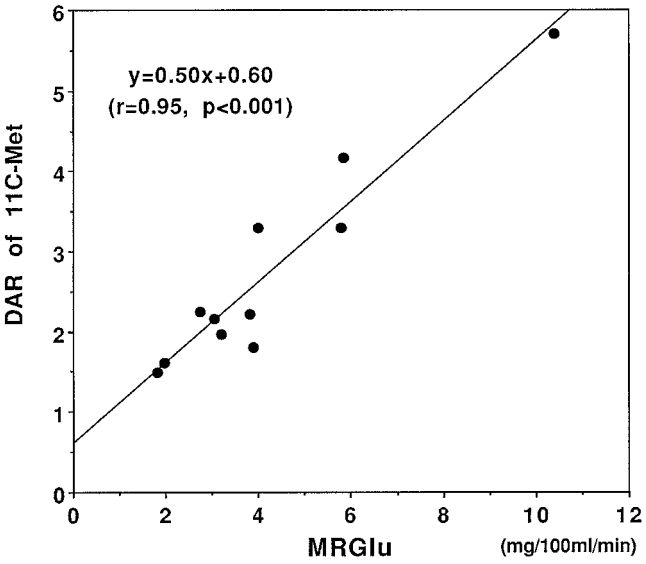

Fig 4. Correlation between metabolic rate for glucose (*MRGlu*) and differential absorption ratio (*DAR*) of L-methyl-^{11}C-methionine (*11C-Met*) in tumor tissue.

A few earlier studies have compared FDG and ^{11}C-methionine as PET tracers for tumors (8–10). Kubota et al (9) reported the usefulness of both tracers for the differential diagnosis of lung tumors and found no significant differences between them. Lindholm et al (10) reported a good correlation of the uptake rates for FDG and ^{11}C-methionine in head and neck cancer. This study also showed a good correlation between the MRGlu and DAR values for tumor tissue. A metabolic demand for glucose and amino acids in malignant tumors that is higher than in normal tissue has been proved by both in vitro and in vivo experiments (34–36). Therefore, a high uptake of both tracers in tumor tissue may reflect a high proliferation rate. Although there are some limitations to applying both tracers for distinguishing tumors from nontumorous lesions (37–39), PET with both tracers appears to be clinically useful for the evaluation of brain tumors, as are CT and MR imaging.

In conclusion, PET with FDG is useful for detecting malignant tumor foci, and PET with ^{11}C-methionine is useful for the delineation of tumor extent. Therefore, PET with FDG and PET with ^{11}C-methionine play a complementary role in the evaluation of brain tumors, particularly

malignant gliomas and their heterogeneous histology.

Acknowledgments

We thank Yoshitaka Tozawa, BS, for photographic assistance.

References

1. Di Chiro G, DeLaPaz RL, Brooks RA, et al. Glucose utilization of cerebral gliomas measured by ^{18}F fluorodeoxyglucose and positron emission tomography. *Neurology* 1982;32:1323–1329
2. Ito M, Lammertsma AA, Wise RJS, et al. Measurement of regional cerebral blood flow and oxygen utilization in patients with cerebral tumors using ^{15}O and positron emission tomography: analytical techniques and preliminary results. *Neuroradiology* 1982;23:63–74
3. Hübner KF, Purvis JT, Mahaley SM, et al. Brain tumor imaging by positron emission computed tomography using ^{11}C-labeled amino acids. *J Comput Assist Tomogr* 1982;6:544–550
4. Bergström M, Collins VP, Ehrin E, et al. Discrepancies in brain tumor extent as shown by computed tomography and positron emission tomography using [^{68}Ga]EDTA, [^{11}C]glucose, and [^{11}C]methionine. *J Comput Assist Tomogr* 1983;7:1062–1066
5. Lilja A, Bergström M, Hartvig P, et al. Dynamic study of supratentorial gliomas with L-methyl-^{11}C-methionine and positron emission tomography. *AJNR Am J Neuroradiol* 1985;6:505–515
6. Shishido F, Murakami M, Miura S, et al. Clinical investigation of ^{18}F-fluorophenylalnine for brain tumor imaging: comparison with ^{11}C-methionine. *Kaku Igaku* 1988;25:1431–1435
7. Wienhard K, Herholz K, Coenen HH, et al. Increased amino acid transport into brain tumors measured by PET of L-(2-^{18}F)fluorotyrosine. *J Nucl Med* 1991;32:1338–1346
8. Daemen BJG, Zwertbroek R, Elsinga PH, Paans AMJ, Doorenbos H, Vaalburg W. PET studies with L-[1-^{11}C]tyrosine, L-[methyl-^{11}C]methionine and ^{18}F-fluorodeoxyglucose in prolactinomas in relation to bromocryptine treatment. *Eur J Nucl Med* 1991;18:453–460
9. Kubota K, Matsuzawa T, Fujiwara T, et al. Differential diagnosis of lung tumor with positron emission tomography: a prospective study. *J Nucl Med* 1990;31:1927–1933
10. Lindholm P, Leskinen-Kallio S, Minn H, et al. Comparison of fluorine-18-fluorodeoxyglucose and carbon-11-methionine in head and neck cancer. *J Nucl Med* 1993;34:1711–1716
11. Ogawa T, Kanno I, Shishido F, et al. Clinical value of PET with ^{18}F-fluorodeoxyglucose and L-methyl-^{11}C-methionine for diagnosis of recurrent brain tumor and radiation injury. *Acta Radiol* 1991;32:197–202
12. Iida H, Miura S, Kanno I, et al. Design and evaluation of Headtome IV, a whole body positron emission tomograph. *IEEE Trans Nucl Sci* 1989;37:1006–1010
13. Ogawa T, Inugami A, Yamaguchi T, et al. A method of obtaining accurate correlation between the positron emission tomogram and the x-ray computed tomogram. *Kaku Igaku* 1985;22:907–911
14. Miura S, Kanno I, Iida H, et al. Anatomical adjustments in brain positron emission tomography using CT images. *J Comput Assist Tomogr* 1988;12:363–367
15. Phelps ME, Huang SC, Hoffman EJ, Selin C, Sokoloff L, Kuhl DE. Tomographic measurement of local cerebral metabolic rate in human with (F-18)2-fluoro-2-deoxy-D-glucose: validation of method. *Ann Neurol* 1979;6:371–388
16. Reivich M, Alavi A, Wolf A, et al. Glucose metabolic rate kinetic model parameter determination in humans: the lumped constants and rate constants for (^{18}F)fluorodeoxyglucose and (^{11}C)deoxyglucose. *J Cereb Blood Flow Metab* 1985;5:179–192
17. Kubota K, Matsuzawa T, Ito M, et al. Lung tumor imaging by positron emission tomography using C-11 L-methionine. *J Nucl Med* 1985;26:37–42
18. Di Chiro G. Positron emission tomography using [^{18}F]fluorodeoxyglucose in brain tumors: a powerful diagnostic and prognostic tool. *Invest Radiol* 1987;22:360–371
19. Patronas NJ, Di Chiro G, Kufta C, et al. Prediction of survival in glioma patients by means of positron emission tomography. *J Neurosurg* 1985;62:816–822
20. Ogawa T, Uemura K, Shishido F, et al. Changes of cerebral blood flow, and oxygen and glucose metabolism following radiochemotherapy of gliomas: a PET study. *J Comput Assist Tomogr* 1988;12:290–297
21. Francavilla T, Miletich RS, Di Chiro G, Patronas NJ, Rizzoli HV, Wright DC. Positron emission tomography in detection of malignant degeneration of low-grade gliomas. *Neurosurgery* 1989;24:1–5
22. Patronas N, Di Chiro G, Brooks RA, et al. Work in progress: (^{18}F)fluorodeoxyglucose and positron emission tomography in the evaluation of radiation necrosis of the brain. *Radiology* 1982;144:885–889
23. Di Chiro G, Oldfield E, Wright DC, et al. Cerebral necrosis after radiotherapy and/or intraarterial chemotherapy for brain tumors. PET and neuropathological studies. *AJNR Am J Neuroradiol* 1987;8:1083–1091
24. Ogawa T, Uemura K, Shishido F, et al. Delayed radiation necrosis of brain evaluated by positron emission tomography. *Tohoku J Exp Med* 1988;155:247–260
25. Valk PE, Budinger TF, Levin VA, Silver P, Gutin PH, Doyle WK. PET of malignant cerebral tumors after interstitial brachytherapy. *J Neurosurg* 1988;69:830–838
26. Hanson MW, Glantz MJ, Hoffman JM, et al. FDG-PET in the selection of brain lesions for biopsy. *J Comput Assist Tomogr* 1991;15:796–801
27. Burger PC, Kleihues P. Cytologic composition of the untreated glioblastoma with implications for evaluation of needle biopsy. *Cancer* 1989;63:2014–2023
28. Dean BL, Drayer BP, Bird CR, et al. Gliomas: classification with MR imaging. *Radiology* 1990;174:411–415
29. Herholz K, Pietryzyk U, Voges J, et al. Correlation of glucose consumption and tumor cell density in astrocytoma: a stereotactic PET study. *J Neurosurg* 1993;79:853–858
30. Mosskin M, von Holst H, Bergström M, et al. Positron emission tomography with ^{11}C-methionine and computed tomography of intracranial tumors compared with histopathologic examination of multiple biopsies. *Acta Radiol* 1987;28:673–681
31. Mosskin M, Ericson K, Hindmarsh H, et al. Positron emission tomography compared with magnetic resonance imaging and computed tomography in supratentorial gliomas using multiple stereotactic biopsies as reference. *Acta Radiol* 1989;30:225–232
32. Ogawa T, Shishido F, Kanno I, et al. Cerebral glioma: evaluation with methionine PET. *Radiology* 1993;186:45–53
33. Kelly PJ, Daumas-Duport C, Kispert DB, et al. Imaging-based stereotaxic serial biopsies in untreated intracranial glial neoplasms. *J Neurosurg* 1987;66:865–874
34. Warburg O. On the origin of cancer cells. *Science* 1956;123:309–314
35. Busch H, Davis JR, Honig GR, Anderson DC, Nair PV, Nyhan WL. The uptake of a variety of amino acids into nuclear proteins of tumors and other tissues. *Cancer Res* 1959;19:1030–1039

36. Issellbacher KJ. Increased uptake of amino acids and 2-deoxy-D-glucose by virus-transformed cells in culture. *Proc Natl Acad Sci U S A* 1972;69:585–589
37. Sasaki M, Ichiya Y, Kuwabara Y, et al. Clinical image: ring-like uptake of [^{18}F]FDG in brain abscess: a PET study. *J Comput Assist Tomogr* 1990;14:486–487
38. Ishii K, Ogawa T, Hatazawa J, et al. High L-methyl-[^{11}C]methionine uptake in brain abscess: a PET study. *J Comput Assist Tomogr* 1993;17:660–661
39. Dethy S, Goldman S, Blecic S, Luxen A, Levivier M, Hildebrand J. Carbon-11-methionine and fluorine-18-FDG PET study in brain hematoma. *J Nucl Med* 1994;35:1162–1166